Energy consumption minimization for a solar lime calciner operating in a concentrated solar power plant for thermal energy storage

Pilar Lisbona[a], Manuel Bailera[b], Thomas Hills[c], Mark Sceats[c], Luis I. Díez[b], and Luis M. Romeo[b]

[a] Fundación Agencia Aragonesa para la Investigación y el Desarrollo (ARAID), Zaragoza, Spain
[b] Escuela de Ingeniería y Arquitectura, Universidad de Zaragoza, Zaragoza, Spain,
[c] Calix Europe (UK) Limited, Salisbury, United Kingdom.

Abstract:

Calcium-looping systems can be integrated in concentrated solar power (CSP) plants as an alternative for thermal energy storage. This storage concept is based in the high temperature reversible calcination-carbonation reactions, in which limestone and lime are alternatively converted. Energy from CSP can be stored by limestone calcination (endothermic reaction) at high temperatures producing pure streams of CaO and CO_2. This energy can be later released when demand increases by means of carbonation reaction (exothermic) at relatively high temperatures.

Calciner reactor is a complex system where heterogeneous chemical reactions take place while absorbing heat from solar concentrating equipment. It is a key element of the process. Depending on the design and the distribution of heat along the calciner, the amount of energy required to store the same amount of chemical energy in the form of lime varies, as well as the temperature of the solids. Optimal design and operating conditions will minimize average temperature in the calciner for a given flow of produced lime. In this work, the modelling of a multi-stage solar calciner is described in the frame of a new solar-based CSP plant.

Keywords:

Ca-looping; Thermal Storage; Solar Calciner; Concentrated Solar Power.

1. Introduction

Increasing rates of electricity generation by variable renewable sources require the deployment of efficient technologies for energy storage. The integration of these storage systems is necessary to match the renewable energy availability with the electricity demand.

A significant number of concentrated solar power (CSP) plants are expected to be commissioned and started up worldwide in a mid-term. According to [1], it is estimated that 7% of global electricity will be produced in CSP plants by 2030, and 25% by the year 2050. So far, most of existing units are installed at United States and Spain, but there are also some units at Italy, Morocco, Algeria, Egypt and South Africa [2]. Developing economies like China and India are undertaking important investments in renewable energy technologies, and solar-based electricity is also included in the framework.

CSP plants allow the use of a renewable energy source for large-scale electricity generation, which can be firmly delivered by the integration of energy storage systems and/or hybrid generation supplies [1]. Most of existing CSP plants runs today according to two main arrangements: parabolic through collectors (PTC) and solar power towers (SPT). Concentration ratios are higher for SPT systems, and then fluid temperatures and efficiencies. On the other hand, PTC usually requires lower investment costs and lower ground surfaces.

In order to increase the number of operating hours and decouple the solar energy availability and the power production, thermal energy storage systems are sometimes included in CSP plants. Medium-to-high temperature levels are selected for those energy storages, in order to increase the round-trip efficiencies. The use of molten salts is the dominant solution at a commercial status [3]; thermal storage capacity ranges from 7.5 to 9 hours of operation. Other materials are also being studied for large-scale thermal energy applications, like natural rocks, recycled ceramics and PCM's [4][5].

Integration of thermochemical energy storage (TCES) has been also proposed as an alternative to increase the flexibility of CSP plants [6]. The performance of these systems relies on endothermic/exothermic inverse chemical reactions. Solar energy is used to provide the heat needed for the endothermic stage, storing the resulting products. When power is demanded, the stored materials are used for the exothermic stage and heat is released to a power cycle. The major advantage of this alternative is the larger storage densities. Calcination/carbonation reactions ($CaCO_3 \leftrightarrow CaO + CO_2$) are really suitable for this purpose, due to its energy density (around 3.2 GJ/m^3) and the large availability of limestones along with their low price.

The application of the calcium-looping (Ca-L) process has been modelled and experimented for a range of unit scales aimed to CO_2 capture [7–9], based on the reversible CaO carbonation / $CaCO_3$ calcination reactions (R.1).

$$CaCO_3 \leftrightarrow CaO + CO_2 \quad \text{(R.1)}$$

A similar concept can be also conceived for concentrated solar power plants to storage energy [10,11]. Solar energy can be used to produce the limestone calcination at high temperature (endothermic reaction), releasing and storing lime and CO_2. This chemical energy stored as lime can be used when required to release heat by the lime carbonation with CO_2 (exothermic reaction), at lower temperature –but still high enough– than the calcination one. The temperature, near to 900°C (equilibrium temperature under a given CO_2 partial pressure of 1 atm) fits in the desirable range of high temperatures potentially attainable in SPT units. This relevant feature would allow for a more efficient generation of electricity from stored energy, thus overcoming the current limitation of temperature imposed by the degradation of molten salts employed in commercial CSP plants [12,13]. Power can be then produced by a Rankine cycle or other thermal engines with higher efficiencies [10,11]. According to these references, good efficiencies can be achieved using Rankine cycles (35.5 %), combined cycles (39 %) or closed Joule-Brayton cycles (42 %).

To actually get these numbers, important challenges arise as concerns the design and operation modes of the reactors involved, calciner and carbonator. Constrains related to the specifics of the solar energy availability and the overall processes integration (calciner/ storage/ carbonation/ power) have to be accounted for, leading to different conditions to those modelled and tested for CO_2 capture systems.

In this paper, the modelling of a calciner operating in a CSP plant is addressed and the results discussed. Despite several works have previously reported the modelling of calciner reactors for CO_2 capture by Ca-L [14,15], the approach is here different since the heat source for limestone calcination is the solar energy. The system proposed is a multi-stage solar calciner. The target is to determine the operating conditions aiming at optimizing the efficiency and the average sorption capacity, by discussing the influence of temperature distribution, as well as solar the heat flux provided in each block.

2. Calcium-looping as energy storage technology

When applied as energy storage technology, the Ca-L process starts with the decomposition of $CaCO_3$ in the calcination reactor (endothermic process) producing CaO and CO_2. A high energy input is required to increase the temperature of inlet streams up to the value required for the calcination reaction. Calcination occurs at a fast rate, which is essentially determined by the CO_2 equilibirum [16]. CaO and CO_2 streams are stored at ambient temperature for their use afterwards as a function of demand once sensible heat is recovered. Storage of the products could be prolonged to weeks or even months as depending on storage conditions and energy demand [17]. The reactants are recirculated into a carbonator reactor where chemical energy is released through the carbonation reaction when energy is demanded.

Important reviews of this concept have been previously published [18][19][20]. There is a general agreement about that carbonate systems are an economically viable option as future thermal energy storage system if their cyclic stability and reversibility are improved. Additional challenges of the technology included in the reviews are: a low thermal conductivity of the sorbents, its agglomeration disposition causing the carbonation to slow down and the difficulty in the design of the reactors and an efficient integration [18]. The two last challenges are also mentioned [19] as main factors that determined the heat storage performance, having the reactors design an important role in the establishment of a reliable energy charging and releasing energy process.

Calcium-looping was proposed for thermal energy storage using oxy-fired circulating fluidized beds due to the large circulation flows of high temperature solids [21]. Most concepts were focused on systems that involve CO_2 capture and were applied to improve flexibility, to increase low capacity factors [22] or to work on peaks and off-peaks times [23]. Several years before, Edwards and Materic [24] published a work about calcium looping in solar power generation plants. Their proposal included a solar calciner and a pressurised fluidised bed carbonator feeding a gas turbine in an open Brayton cycle. Simulation results showed electric efficiencies of 40–50% with sorbent carbonation activities between 15% and 40%. This was the basis for the concept developed with circulating fluidized beds and based on a population balance model on sorbent particles, and introducing the novelty of the cyclic operation of the system [25] and some experimental work for demonstration [26]. Modelling outcomes showed the feasibility of the concept with CO_2 capture efficiency of 90% when the residence time of the recirculated sorbent around 200 s. Experimental results highlighted the importance of controlling temperature non-uniformities and avoid peak temperatures to prevent early deactivation and preserve long term CO_2 uptake sorbent capacity [26]. Moreover, they concluded that an exceedingly large radiative flux may cause excessive overheating increasing sorbent deactivation. For these reasons, the design of the calciner is one of the key elements in the system. An optimal fluidisation was proposed to control surface overheating and avoids peak temperatures. As small particles are required for fast calcination it seems more suitable a co-current entrained flow calciner reactor design. There is a lack of research for this calciner design and our work tries to show light about the quantification of the energy fluxes.

In recent years, several integrations of CSP and Ca-looping have been proposed [27] that corroborates the efficiency figures showed above. The use of a closed CO_2 Brayton power cycle to produce directly power -or indirectly by means of a Rankine cycle with reheater- or a supercritical CO_2 Brayton cycle shows high efficiencies, up to 45% [11]. Similar efficiencies are obtained using a pressurized fluidized reactor for carbonation and a closed CO_2 circuit is used for operation of both the CaL process and the power cycle [10]. Operational variables that maximize efficiency include the carbonator pressure and temperature of 3.2 bars and 875ºC, and pressurized CO_2 storage vessel at 75 bar.

Another key variable on the system is the activity level of the sorbent. Improvements in sorbent activity levels do not affect efficiency but capital costs and reductions in the required storage volume [24]. One of the most significant advantages of the CSP–CaL integration is the use of natural limestone as CaO precursor. Limestone is an abundant, non-toxic and cheap material (6-10 €/t), which presents suitable physical properties in the temperature range of interest for CSP thermal energy storage. Nevertheless, CaO from cyclic limestone calcination shows a strong deactivation under CaL specific conditions for CO_2 capture. These conditions involve high calcination temperatures under high CO_2 partial pressure [8]. It is usually assumed that this decay of CaO conversion will also limit the efficiency of the CaL process for TCES [28]. However, the conditions for CSP and for CO_2 capture are different and the loss of activity for CSP is not as relevant as in CO_2 capture conditions. This has been confirmed by a recent thermogravimetric analysis study [29].

In spite of these relevant results, literature looks for sorbent improvements analysing the multicycle activity of the natural $CaCO_3$ minerals [30]; doping and modifying $CaCO_3$ [31] for increasing solar absorptance and heat release [31], pre-processing limestone to enlarge the long-term performance of the sorbent upon iterated cycles [26], and developing synthetic Ca-based materials for energy storage [32].

In any case, the lower calcination temperature, the more limited sintering in the CaO and the higher efficiency of the CaL process. Temperature of calcination will strongly depend on the distribution of heat along the calciner reactor, which is the key issue considered in this work. The main objective is twofold: to avoid any temperature peak in the reactor and to preserve long term CO_2 uptake sorbent capacity. The distribution of the heat required in the calciner is not uniform since it will depend on the temperature inside the reactor and the extent of the calcination reaction. To achieve a similar conversion output in the calciner, different layouts of heat distributions may be applied along the calciner reactor. In this work, calciner is divided in short reactors (around 1.5-2.0 meters) with constant but different heat inputs with the aim of controlling the temperature of the solid inside as a function on the calcination conversion. The assessment of the distribution of the heat fluxes is a key objective of the paper. It will lead to less sintering in the lime particles, faster reactions (lower dimensions required) and minimize calciner energy consumption.

3. Methodology

In the framework of the SOCRATCES project, funded by the European Commission under the H2020 Program, the construction of a pilot solar calciner is one of the specific objectives [33]. The calciner reactor will be a one-stage solar co-current entrained flow reactor which provides heat to the endothermal calcination reaction. The calciner presents cylindrical geometry with an initial height of 9 meters, 43 millimetres of internal diameter and 48 mm outside diameter made of stainless steel. The base case for the feed flowrate of stored $CaCO_3$ into the calciner is 5 kg/h and the gaseous atmosphere in the calciner is considered to be 100% CO_2. Pressure is considered to be constant along the calciner and equals to 1 bar [34].

A thorough model of the calciner has been developed to assess the behaviour of this element under different designs. The calciner model takes geometry, heat transfer and calcination kinetics into account, thus obtaining the temperature profiles along the carbonator under isothermal and non-isothermal conditions. The steady-state model has been implemented in EES (Engineering Equation Solver). Figure 1 illustrates the discretization scheme of the calciner model.

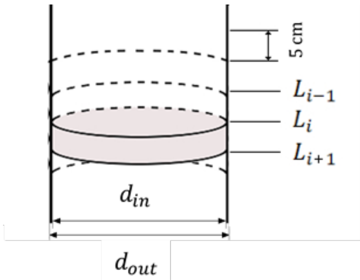

Figure 1. Discretization scheme of the calciner model.

To calculate the residence time of the gas in the carbonator, 1D plug flow is considered. The entraining velocity in downflow for the solid is calculated through the terminal velocity and the gas velocity. The reactor has been discretized in slides of 5 cm length.

3.1. Calcination kinetic model

The Generalised Random Pore Model (GRPM) has been developed by Calix. It combines the random pore models of Bhatia & Perlmutter and Gavalas [35,36] with the shrinking core model described by Borgwardt [37], accounting for overlap through the statistics of pore intersections [38]. In this approach, the reaction front velocity r is the same for reaction in the pores and from the surface. As such, it is no longer necessary to select on or the other model depending on particle size and porosity, and sorbents which experience significant extents of calcination through both mechanisms can be more accurately modelled. The GRPM has been implemented in the calciner model. The evolution of the conversion, $X(t)$, with the residence time of the solid will follow the expression provided in (1).

$$X(t) = \int_0^t r \frac{6 \cdot \left(d_p 2rt\right)^2}{d_p^3} dt + \left(1 - e^{\left(-S_{A0} rt - \pi L_{A0} (rt)^2\right)}\right) \int_t^{d_p/2k} r \frac{6 \cdot \left(d_p 2rt\right)^2}{d_p^3} dt \qquad (1)$$

where S_{A0} is the pore surface area calculated as the difference between BET surface area and geometrical surface area and L_{A0} is the mean pore length. A mean particle diameter d_p of 60 microns was used.

In the GRP kinetic model, the calcination reaction rate, r [m/s], is the fitting parameter of conversion calculation through (1) to the experimental data. The reaction rate is given by (2) when the atmosphere in the calciner is pure CO_2 [39].

$$r = k_o \cdot e^{\left(-\frac{E_a}{\mathcal{R}T}\right)} \cdot (1 - \theta_{CO2})^{N_v} \cdot \left(1 - \frac{P_{CO2}}{P_{CO2,eq}}\right) \qquad (2)$$

where k_o is the pre-exponential factor, E_a is the activation energy, N_v is considered to take the value of 1 for limestone and θ_{CO2} is based on the Langmuir isotherm, defined through (3) where the saturation pressure is taken to be the equilibrium pressure.

$$\theta_{CO2} = \frac{\frac{P_{CO2}}{P_{CO2,eq}}}{\left(1 + \frac{P_{CO2}}{P_{CO2,eq}}\right)} \tag{3}$$

The kinetic model allows for computing the conversion of each component as a function of time, t. Therefore, to characterize the mass flows of different components, it is required to know the temperature, the residence time of solid and the gas in the reactor. The GRP calcination kinetic model has been implemented in the EES overall model of the multi-stage solar calciner whose results are presented in this manuscript.

3.2 Residence time for the solids

The time of interaction between the solid and the gas is limited to the residence time of the solid in the calciner since its terminal velocity must be also accounted. For those flows with Reynolds lower than 2 and small size particles, the following (4) may be applied for the downward velocity of single particles, v_s, (concentration of particles is assumed diluted) [40]:

$$v_s = v_{s,i} \cdot e^{-bt_s} + \left(v_g + v_t\right) \cdot (1 - e^{-bt_s}) \tag{4}$$

where $v_{s,i}$ is the initial velocity of the solid, v_g is the velocity of the gas phase, and v_t is the terminal settling velocity of the particle in a static fluid. The parameter b, and the velocity v_t are given by (5) and (6):

$$b = \frac{18\mu}{\rho_s d_p^2} \tag{5}$$

$$v_t = \frac{\left(\rho_s + \rho_g\right) d_p^2 g}{18\mu} \tag{6}$$

where μ is the viscosity of the gas, ρ_s is the density of the solid, ρ_g is the density of the gas, d_p is the diameter of the solid particles, and g the gravity.

The integration of (4) provides the relationship between the calciner length and the residence time of the solids (7).

$$L = \int_0^{t_{s,L}} v_s dt_s = \frac{v_{s,i}}{b}(1 - e^{-bt_s}) + \left(v_g + v_t\right) \cdot \left(t_s - \frac{1 - e^{-bt_s}}{b}\right) \tag{7}$$

It can be assumed that v_g and μ are constants in the interval of integration for the case of study. Moreover, the variation of v_t with time (due to the variation of ρ_g) can also be neglected when integrating, since $v_g \gg v_t$.

Thus, this can be directly solved by the EES software to compute the residence time of the solid as a function of the length, what will allow determining the mole flows along the reactor as a function of the distance from the entrance.

3.3 Plug flow model (1D) for the gas

The residence time of the gas is given by (8):

$$t_g = \int_0^{V_C} \frac{\pi r_{in}^2}{\dot{V}} dL \quad (8)$$

where r_{in} is the inner radius of the calciner, $\dot{V}$ is the volumetric flow rate, and V_C the calciner volume. Moreover, $\dot{V}$ is the product of the average gas velocity multiplied by the cross-sectional area of the reactor, which in the study case must be corrected by subtracting the area occupied by the solid. The variation in the effective cross-sectional area along the reactor may be neglected as $CaCO_3$ is consumed when CaO is produced.

Besides, it is assumed that the pressure inside the reactor remains constant. Hence, the volumetric flow rate is given by (9), according to the ideal gas law:

$$\dot{V}_{L2} = \frac{(1 + X_{L2}) \cdot T_{L2}}{T_{L1}} \dot{V}_{L1} \quad (9)$$

The residence time of the gas, through a length L_i in which $\dot{V}_{Li}$ can be considered constant will be $t_{g(L1)} = L_i \cdot S_{eff}/\dot{V}_{Li}$.

3.4 Heat transfer model

The following steps are taken to compute the heat transfer to the cloud of gas and particles to the cooling fluid. First, an energy balance inside the reactor is computed for each slice of reactor (from length L_{i-1} to length L_i) by (10):

$$\sum_{\substack{j=CaO,\\ CO2,\\ CaCO3}} Cp_j \cdot \dot{n}_{j,L_i} \cdot \left(T_{L_i} - T_{L_{i-1}}\right) = \Delta H_r \cdot \left(\dot{n}_{CaCO3,L_i} - \dot{n}_{CaCO3,L_{i-1}}\right) + \dot{q}'_{L_i} \cdot (L_i - L_{i-1}) \quad (10)$$

where Cp_j and $\dot{n}_{j,}$ are the specific heat and mole flow rate of component j, respectively, T is the temperature of the cloud of gas and particles (which is assumed homogeneous inside the carbonator), ΔH_r is the heat of reaction (178 kJ/mol), and $\dot{q}'_{L_i}$ is the heat flow throughout the inside wall of the carbonator per unit of length. The latter accounts for radiation and convection, in the form of (11):

$$\dot{q}'_{L_i} = \dot{q}'_{rad,L_i} + \dot{q}'_{conv,L_i} \tag{11}$$

$$\dot{q}'_{rad,L_i} = \frac{\varepsilon_w}{\alpha_{g+p} + \varepsilon_w - \alpha_{g+p} \cdot \varepsilon_w} \cdot \sigma \cdot (\varepsilon_{g+p} \cdot T^4_{iw,L_i} - \alpha_{g+p} \cdot T^4_{L_i}) \cdot 2\pi r \tag{12}$$

$$\dot{q}'_{conv,L_i} = h_{g,L_i} \cdot \left(T_{iw,L_i} - T_{L_i}\right) \cdot 2\pi r \tag{13}$$

where α_{g+p} and ε_{g+p} are the absorptivity and emissivity of the gas-particle mixture, ε_w the emissivity of the carbonator wall, σ is the Boltzmann's constant, T_{iw} is the temperature of the inner wall of the carbonator, r the inner radius of the carbonator, and h_g the convective coefficient.

Besides, the model for the calculation of the convective coefficient is borne out of 'Heat Transfer' by Nellis G and Klein S [41], and follows (14) to (18):

$$h_{g,L_i} = \frac{Nu_{Li} \cdot k_{Li}}{2r} \tag{14}$$

$$Nu_{L_i} = 3.66 + \frac{\left(0.049 + \frac{0.020}{Pr_{Li}}\right) \cdot Gz_{Li}^{1.12}}{1 + 0.065 \cdot Gz_{Li}^{0.7}} \tag{15}$$

$$Pr_{Li} = \frac{Cp_{Li} \cdot \mu_{Li}}{k_{Li}} \tag{16}$$

$$Gz_{Li} = \frac{Re_{Li} \cdot Pr_{Li}}{L/2r} \tag{17}$$

$$Re_{Li} = \frac{4 \cdot \dot{m}_{Li}}{\pi \cdot 2r \cdot \mu_{Li}} \tag{18}$$

where Nu is the Nusselt number, k the thermal conductivity, Pr the Prandtl number, Gz the Graetz number, μ the viscosity, Re the Reynolds number, and $\dot{m}$ the mass flow rate.

The temperature of the outer wall of the calciner, T_{ow}, is computed by the formula of heat conduction through a tube wall, given by (19):

$$\dot{q}'_{L_i} = \frac{T_{ow,L_i} - T_{iw,L_i}}{R_{tube} \cdot L_i} \tag{19}$$

$$R_{tube} = \frac{\ln(\frac{r_{out}}{r})}{2\pi \cdot k_{tube} \cdot L_i} \tag{20}$$

where R_{tube} (20) is the thermal resistance of the carbonator tube, r_{out} the outer radius of the calciner, and k_{tube} the thermal conductivity of the calciner tube (0.025 kW/m·K).

4. Results

Prior to use the model to obtain realistic results from simulations, the model must be substantiated through validation. The kinetic model for calcination presented in section 3.1 was validated through TGA experimental tests by Calix in the range of operation conditions applicable to solar flash calcination, as cited hereinafter. After validation, the first step to estimate the distribution of heat requirements in the calciner for different temperatures is the simulation of isothermal operation in the window of suitable temperature values. The heat requirements obtained under this scenario would represent the minimum heat flow demanded to achieve a specific temperature and a given final conversion. However, its implementation is not feasible and alternative reactor designs must be explored to split the supply of heat.

Once the minimum ideal heat flux requirements were estimated for isothermal operation, two discretized cases which pretend to be closer to a real implementation of the multi-stage solar calciner are proposed and simulated. The objective of the study is to define new designs of the calciner reactor which fulfil three characteristics: (i) achieve high calcination conversion at the outlet of the last calcination stage, (ii) minimize heat consumption and (iii) limit peak temperatures within the reactor below 1000 ºC to allow for the use of conventional steels in the construction of the reactor. The results obtained show the minimum heat requirement for two discretized multi-stage reactors to achieve equivalent final conversions. Finally, a short summary of the implications which these results would have in the design of a multi-stage solar reactor is presented to close the section.

4.1. Validation of the kinetic model

The Generalised Random Pore Model (GRPM) developed by Calix to describe the kinetic of the calcination reaction was validated with experimental data [42]. These experimental values were obtained for isothermal conditions at about 950ºC in a fluidised bed. The model presented excellent agreement between prediction and experimental kinetic data under 957 ºC and 10% steam calcination conditions. The model proposed is able to predict the calcination conversion of the sorbent in a range of conditions of interest for the CaL energy storage process.

4.2. Isothermal operation

The demand of heat per length unit required to maintain constant temperature in the calciner has been first calculated in the simulations. These values will be used to define the heat flux pattern introduced along the calciner and the total heat power. The following cases implement the GRP calcination kinetic model and consider isothermal operation. It is important to notice that EES simulations have been run under 100% CO_2 atmosphere while applied GRP model has been adjusted using experimental data obtained under 20% CO_2 in N_2 atmosphere.

The pressure inside the calciner is assumed 1 bar and the simulated temperatures within the reactor vary from 900ºC to 975ºC. The initial mass flowrate of $CaCO_3$ is 5 kg/h. The GRP model provides a more accurate value of conversion profile along the calciner than other models. Thus, it is the most suitable to realistically define the required heat distribution along the calciner, Figure 2.

The calculated residence time of the particles ranges between 28-63 seconds (particle diameter of 60 μm) depending on the temperature (975 ºC-900 ºC) and the corresponding conversion of limestone. The higher the conversion, the higher the production of CO_2 and the higher the velocity of the gas and the solid cloud inside the calciner. The carbonation-calcination equilibrium for a 100% CO_2 atmosphere and atmospheric pressure is achieved at about 895ºC.

The conversion profiles of the calciner are presented in Figure 2 together with required heat flux per unit length. The final conversion varies from 20% to 100% for 900ºC and 950-975ºC respectively. If temperature is kept between 950-975ºC, total conversion is ensured in the calciner outlet under the simulated conditions. Thus, the maximum storage efficiency is achieved in those cases. Total heat power requirement for the cases which achieve complete calcination (100% conversion), 950 ºC and 975 ºC, are 2468 W and 2470 W respectively. These power requirements could correspond to primary solar radiation in the range of 4940 W and 8233 W since the efficiency of solar radiation utilization ranges between 30-50% [34]. These figures should be helpful to size the heliostat field for the specific site of the calciner.

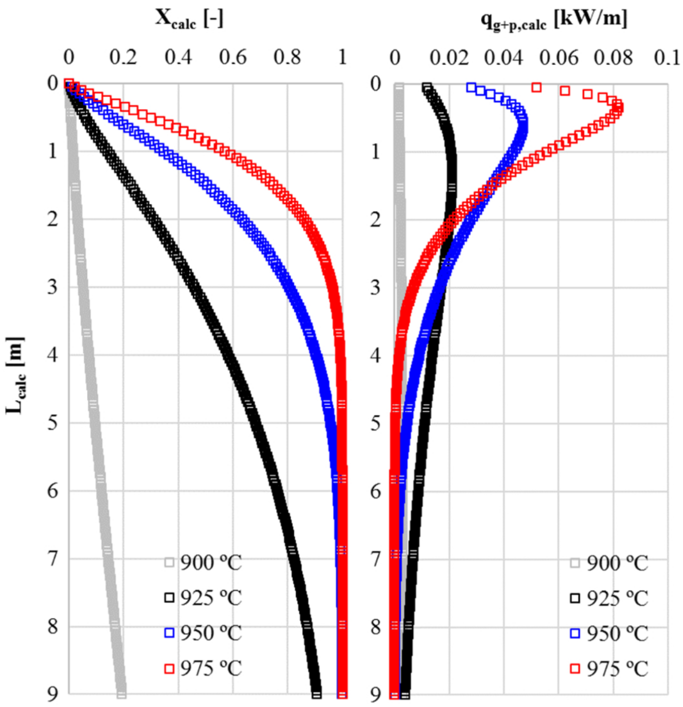

Figure 2. (a) Conversion profiles of the calciner (X) vs. length, (b) required heat per unit length (q) vs. length.

It is also observed that the last meters of the simulated calciner would not be required for temperatures near 950 ºC since calcination reaction velocity is fast enough to ensure total conversion at lengths lower than 7 m. For temperatures around 975 ºC, the length of the calciner could be further reduced down to 2.5-3.5 m to achieve calcination conversions near 100%.

4.3. Multi-stage solar reactor

In a single-stage solar calciner, this kind of distribution of heat will not be achieved and the most probable distribution will be an almost uniform distribution of heat flux along the whole length, i.e. constant value of kW/m. Thus, a division of the reactor must be foreseen and each calciner reactor stage must be designed to receive a different heat input. A first approach of six-stages solar in-series reactors is explored to understand the evolution of needs of heat and assess the efficiency of the system. Then, a three-stages solar reactor is also simulated in order to understand the behavior of this configuration with regard to calcination conversion. The three-stages reactor appear to be more feasible to implement in real designs of solar calciners, in order to not increase a lot the operation complexity.

4.3.1. Six-stages solar reactor

The next proposal of heat distribution in six different elements with uniform heat fluxes pretends to assess the total heat demand while operating at the lowest possible temperature to achieve total calcination. This case study considers an inlet temperature of the $CaCO_3$ from the solar calciner of 895 ºC. The heat power provided to each reactor which have been simulated are distributed in two 6-stages profiles (*profile a*): (i) 1 m 500 W/m, (ii) 1 m 1000 W/m, (iii) 1 m 500 W/m, (iv) 1 m 300 W/m, (v) 2 m 80 W/m, (vi) 1 m 50 W/m, (vii) 2 m without heat input, and (*profile b*): (i) 1 m 790 W/m, (ii) 1 m 810 W/m, (iii) 1 m 500 W/m, (iv) 1 m 300 W/m, (v) 2 m 80 W/m, (vi) 1 m 10 W/m, (vii) 2 m without heat input. These profiles have been guessed from the heat flux distribution obtained in the previous isothermal calculation.

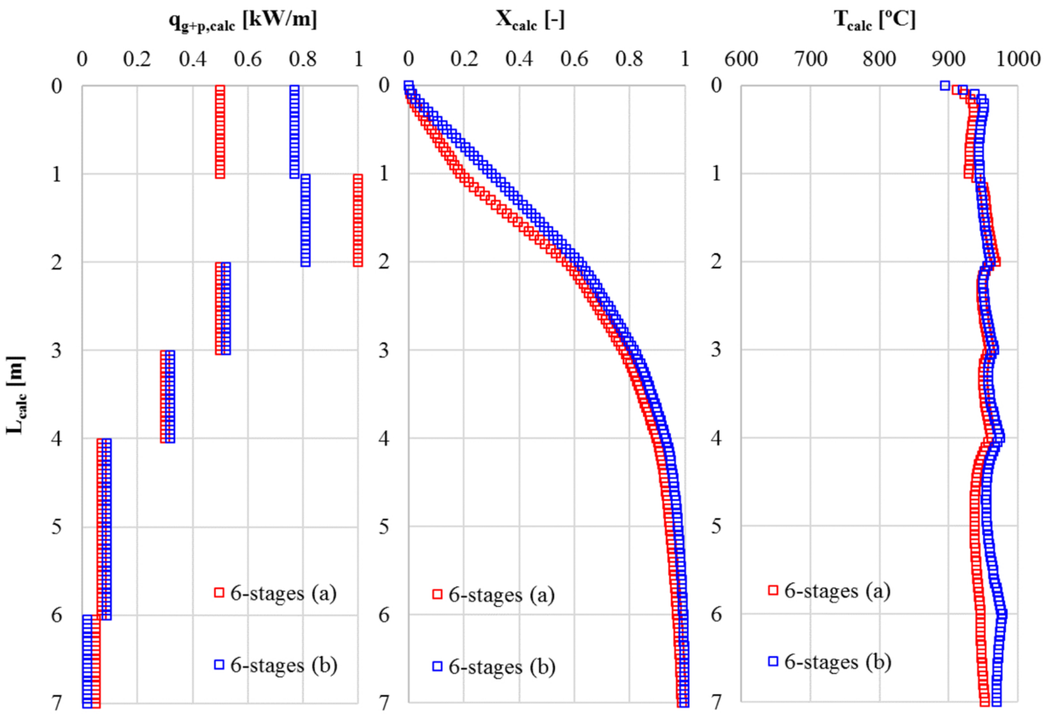

Figure 3. (a) Supplied heat per unit length, (b) Temperature (T) and (c) Conversion profile of the calciner (X) vs. calciner length.

Conversion and temperature profiles along the calciner are shown in Figure 3 (a). These heat supply distributions achieve the total calcination of limestone (ca. 7.0-7.5 meters) without strong temperature peaks and a flat temperature profile around 950ºC (average temperature 945ºC [6-stages (a)] and 960ºC [6-stages (b)]). The total heat powers provided are 2490 W and 2510 W along the six reactors to achieve a 98.4% and 99.9% of calcination conversion respectively. These values are quite similar to those obtained for the ideal isothermal operation. Thus, the six-stage reactor, which discretizes the heat supply, presents a behaviour near to ideal operation but with a difficult manageable configuration.

Figure 3 presents the comparison between both profiles, profiles 6-stages (a) and 6-stages (b), and shows total calcination for both scenarios. Heat supply and temperatures are somehow lower for profile 6-stages (a) and the consequent slower calcination reaction is illustrated in Figure 3. The thermal energy storage efficiencies for each scenario are 97.6% and 98.3%, respectively.

Results show that still high energy storage efficiencies would be achieved for a simplified configuration of a four-stages reactor, in the range of 85-95% depending on the selected heat distribution profile. Therefore, the last two stages could be neglected since their contribution in the increase of energy storage efficiency is quite limited and the total length would be reduced to a maximum of four meters.

4.3.2. Three-stages solar reactor

Although results from six-stage reactor show a suitable performance as for conversion, heat requirements or peak temperatures, the complexity of such number of stages is high. The regulation of six-sections heliostats may be a limiting step for the construction of the proposed design. Thus, the number of stages must be reduced to allow a simplified operation of the concept. This case assesses the behavior of three-stages solar calciners with heat fluxes of (a) 800, 300 and 30 W/m with a length of 2.25 m and (b) 700, 350 and 30 W/m with a length of 2.25 m. The initial temperature considered for the introduced limestone is 895 ºC. Near total conversion of limestone (99.78% and 97.73% for (a) and (b) respectively) is achieved at the outlet of the calciner as observed in Figure 4 (b). The total requirement of heat for these configurations are 2627 W and 2441 W respectively which could correspond up to 8756 W of primary solar radiation, 6% higher than the minimum requirement (isothermal operation). The thermal energy storage efficiencies for each scenario are 93.8% and 98.9%, respectively.

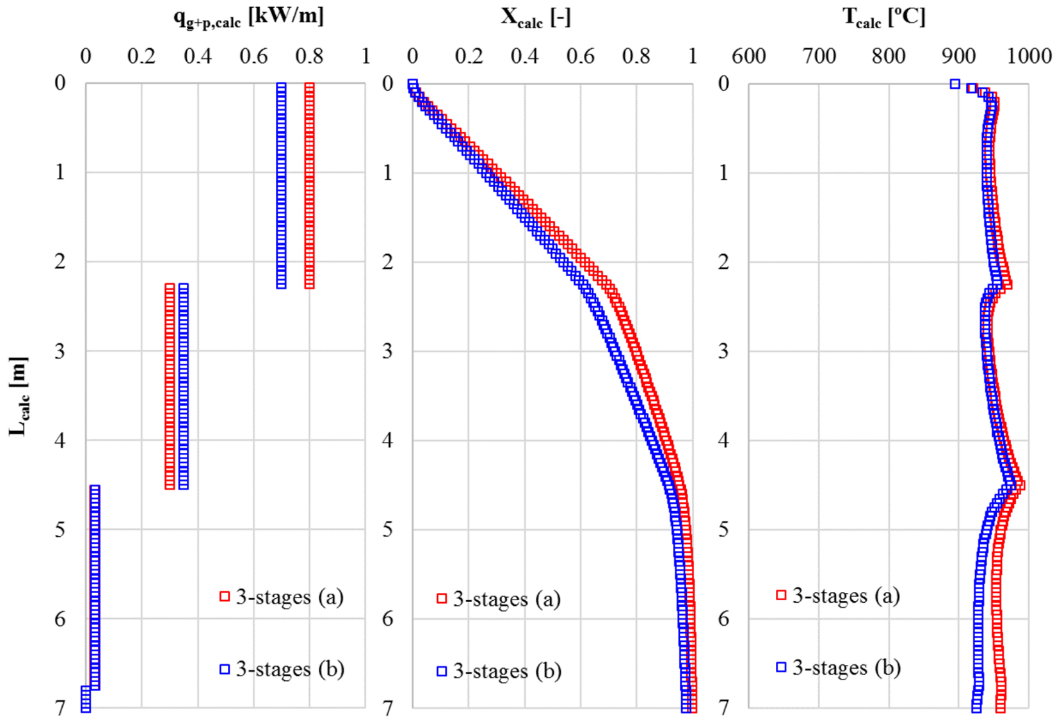

Figure 4. (a) Supplied heat per unit length (q), (b) Temperature (T) and (c) Conversion profile of the calciner (X) vs. calciner length.

Again, results show that significant energy storage efficiencies would be achieved for a simplified configuration of a two-stages reactor, near 90% and 95% for heat distribution profiles (b) and (a) respectively. The last stage could be removed for both profiles since their contribution in the energy storage efficiency is very low. The total length would be limited to four and a half meters and the number of reactors would be more feasible to implement.

4.4. Design implications for multi-stage solar reactor

For the flash calcination of limestone, a one-dimensional model was developed to simulate a constant-heat flow entrained flow reactor. Hodgson et al. validated this kinetic model against data from TGA under representative conditions of operation, and satisfactory agreements were found between them [42].

The established model could provide a theory basis to simulate the multi-stage solar reactor. Similar modelling techniques applied to different low-scale calciners have been proved accurate enough to represent its performance [16][43][44][45]. Our results showed that the optimal temperatures of operation for complete calcination are in the range of 950-975 ºC, which are also suitable for materials.

The lower the number of reactors, the lower the capital costs of the multi-stage solar reactor. Thus, a proper separation of the required heat flow, which also account for the limitations of real design would include two 2.5-meters entrained flow reactors with heat fluxes of 0.8 kW/m and 0.3 kW/m respectively. The proposed configuration will present a hot spot temperature at the outlet of the second reactor as illustrated in Figure 4. This could be avoided with a slightly shorter design of the second stage reactor, also reporting a minor reduction of energy storage efficiency.

5. Conclusions

This paper compares and analyses the behaviour of a one-stage isothermal calciner and two multi-stage solar calcination reactors under different situations with the target of achieving the highest possible energy storage efficiency and to limit the peak temperatures within the reactors. The highest possible energy storage efficiency is related to the highest calcination conversion in the reactor while the lowest possible temperatures are required to limit sintering of lime, to maintain the sorption capacity of the cycled material and to allow for the utilization of more economic steels.

Results obtained for the isothermal reactor provide the best possible energy storage efficiency for a given temperature since the required heat is supplied at each point of the reactor. This is an ideal configuration which cannot be implemented but provides the lower threshold of heat required for full calcination for each operating temperature. The total heat demanded for a six-stage calciner with constant heat flows per stage would be similar to the values calculated for isothermal operation and lead to high storage efficiencies. However, the complexity of implementing six-stages of a solar calciner makes mandatory the reduction of the number of stage sacrificing some points of storage efficiency. It must also be considered that the fewer stages in the calciner, the lower capital expenditure (CAPEX) of this element.

Two heat flow profiles were proposed for the multi-stage calciners in order to observe differences in the resulting temperatures. Obtained results show that multi-stage designs which operates at lower heat flux inputs may be more interesting since peak temperature are reduced in the profile of temperatures. The maximum temperatures for 6-stages solar calcination reactor were limited to 978ºC while the peak temperature for 3-stages solar calcination reactor was 993 ºC. Energy consumption minimization is achieved with a design that includes two 2.5-meters entrained bed reactors with heat fluxes of 0.8 kW/m and 0.3

kW/m respectively. Although final conversion of limestone is somehow limited in these situations (around 97%), the final efficiency of solar thermal energy storage may even be higher. However, the major advantage of these designs will be related to the milder temperature distribution along the different stages of the calciner reactor.

Acknowledgments

The research leading to these results has received funding from the European Union Horizon 2020 research and innovation programme under grant agreement No 727348, project SOCRATCES.

Nomenclature

Variables:

b calculation parameter, 1/s

Cp specific heat, kJ/(kmol·K)

d diameter, m

E_a calcination activation energy, kJ/mol

g gravity, m/s^2

Gz Graetz number, -

h convective heat transfer coefficient, kW/(m^2·K)

k thermal conductivity, kW/(m·K)

k_0 pre-exponential factor, m/s

L length, m

L_{A0} pore surface area, m^2/m^3

$\dot{m}$ mass flow rate, kg/s

$\dot{n}$ mole flow rate, kmol/s

Nu Nusselt number, -

P pressure, bar

Pr Prandtl number, -

$\dot{q}'$ heat flux per unit of length, kW/m

r reaction front velocity, m/s

r radius, m

R thermal resistance, K/kW

$\mathcal{R}$ ideal gas constant, kJ/(kmol·K)

S_{A0} pore surface area, m^2/m^3

S_{eff} effective cross-sectional area of reactor, m^2

t reacting time or residence time, s

T temperature, K

v velocity, m/s

V volume, m^3

$\dot{V}$ volumetric flow rate, m^3/s

X conversion, -

ΔH_r enthalpy of calcination, kJ/kmol

Greek symbols

α	absorptivity, -
ε	emissivity, -
θ	*GRPM* kinetic parameter, -
μ	viscosity, kg/(m·s)
ρ	density, kg/m^3
σ	Stefan-Boltzmann constant, kW/(m^2·K^4)

Subscripts and superscripts

c	calciner
$conv$	convection
eq	equilibrium
g	gas
i	initial value or discretization index for axial position
iw	inner wall
j	component j
L	covered length
out	outer radius or diameter
ow	outer wall
p	particle
rad	radiation
s	solid
t	terminal velocity
$tube$	calciner tube
w	wall

References

[1] Islam MT, Huda N, Abdullah AB, Saidur R. A comprehensive review of state-of-the-art concentrating solar power (CSP) technologies: Current status and research trends. Renew Sustain Energy Rev 2018;91:987–1018. doi:10.1016/j.rser.2018.04.097.

[2] SolarPACES. CSP projects around the world. 2019. http://www.solarpaces.org/csp-technology/csp-projects-around-the-world/.

[3] Kearney D, Kelly B, Herrmann U, Cable R, Pacheco J, Mahoney R, et al. Engineering aspects of a molten salt heat transfer fluid in a trough solar field. Energy 2004;29:861–70. doi:10.1016/S0360-5442(03)00191-9.

[4] Kuravi S, Trahan J, Goswami DY, Rahman MM, Stefanakos EK. Thermal energy storage technologies and systems for concentrating solar power plants. vol. 39. 2013. doi:10.1016/j.pecs.2013.02.001.

[5] Xu B, Li P, Chan C. Application of phase change materials for thermal energy storage in concentrated solar thermal power plants: A review to recent developments. Appl Energy 2015;160:286–307. doi:10.1016/j.apenergy.2015.09.016.

[6] Kyaw K, Matsuda H HM. Applicability of carbonation/decarbonation reactions to high-temperature thermal energy storage and temperature upgrading. J Chem Eng Jpn 1996;29:119–25.

[7] Romeo LM, Abanades JC, Escosa JM, Paño J, Giménez A, Sánchez-Biezma A, et al. Oxyfuel carbonation/calcination cycle for low cost CO2 capture in existing power plants. Energy Convers Manag 2008;49. doi:10.1016/j.enconman.2008.03.022.

[8] Perejón A, Romeo LM, Lara Y, Lisbona P, Martínez A, Valverde JM. The Calcium-Looping technology for CO2 capture: On the important roles of energy integration and sorbent behavior. Appl Energy 2016;162. doi:10.1016/j.apenergy.2015.10.121.

[9] Lisbona P, Martínez A, Lara Y, Romeo LM. Integration of carbonate CO2 capture cycle and coal-fired power plants. A comparative study for different sorbents. Energy and Fuels 2010;24:728–36. doi:10.1021/ef900740p.

[10] Chacartegui R, Alovisio A, Ortiz C, Valverde JM, Verda V, Becerra JA. Thermochemical energy storage of concentrated solar power by integration of the calcium looping process and a CO 2 power cycle. Appl Energy 2016;173:589–605. doi:10.1016/j.apenergy.2016.04.053.

[11] Ortiz C, Chacartegui R, Valverde JM, Alovisio A, Becerra JA. Power cycles integration in concentrated solar power plants with energy storage based on calcium looping. Energy Convers Manag 2017;149:815–29. doi:10.1016/j.enconman.2017.03.029.

[12] Peng Q, Yang X, Ding J, Wei X, Yang J. Design of new molten salt thermal energy storage material for solar thermal power plant. Appl Energy 2013;112:682–9. doi:10.1016/j.apenergy.2012.10.048.

[13] Peng Q, Ding J, Wei X, Yang J, Yang X. The preparation and properties of multi-component molten salts. Appl Energy 2010;87:2812–7. doi:10.1016/j.apenergy.2009.06.022.

[14] Parkkinen J, Myöhänen K, Carlos J, Arias B. Modelling a calciner with high inlet oxygen concentration for a calcium looping process. Energy Procedia 2017;114:242–9. doi:10.1016/j.egypro.2017.03.1166.

[15] Martínez I, Grasa G, Parkkinen J, Tynjälä T, Hyppänen T, Murillo R, et al. Review and research needs of Ca-Looping systems modelling for post-combustion CO 2 capture applications. Int J Greenh Gas Control 2016;50:271–304. doi:10.1016/j.ijggc.2016.04.002.

[16] Rodriguez N, Alonso M, Grasa G, Abanades JC. Heat requirements in a calciner of CaCO3

integrated in a CO2 capture system using CaO 2008;138:148–54. doi:10.1016/j.cej.2007.06.005.

[17] Luo L, Tsoukpoe KEN, Liu H, Pierre N Le. A review on long-term sorption solar energy storage 2009;13:2385–96. doi:10.1016/j.rser.2009.05.008.

[18] Khosa AA, Xu T, Xia BQ, Yan J, Zhao CY. Technological challenges and industrial applications of CaCO3/CaO based thermal energy storage system – A review. Sol Energy 2019. doi:10.1016/j.solener.2019.10.003.

[19] Chen X, Zhang Z, Qi C, Ling X, Peng H. State of the art on the high-temperature thermochemical energy storage systems. Energy Convers Manag 2018. doi:10.1016/j.enconman.2018.10.011.

[20] Sunku Prasad J, Muthukumar P, Desai F, Basu DN, Rahman MM. A critical review of high-temperature reversible thermochemical energy storage systems. Appl Energy 2019. doi:10.1016/j.apenergy.2019.113733.

[21] Arias B, Criado YA, Sanchez-Biezma A, Abanades JC. Oxy-fired fluidized bed combustors with a flexible power output using circulating solids for thermal energy storage. Appl Energy 2014. doi:10.1016/j.apenergy.2014.06.074.

[22] Astolfi M, De Lena E, Romano MC. Improved flexibility and economics of Calcium Looping power plants by thermochemical energy storage. Int J Greenh Gas Control 2019. doi:10.1016/j.ijggc.2019.01.023.

[23] Zhou L, Duan L, Anthony EJ. A calcium looping process for simultaneous CO 2 capture and peak shaving in a coal-fired power plant. Appl Energy 2019. doi:10.1016/j.apenergy.2018.10.138.

[24] Edwards SEB, Materić V. Calcium looping in solar power generation plants. Sol Energy 2012. doi:10.1016/j.solener.2012.05.019.

[25] Tregambi C, Montagnaro F, Salatino P, Solimene R. A model of integrated calcium looping for CO<inf>2</inf> capture and concentrated solar power. Sol Energy 2015. doi:10.1016/j.solener.2015.07.017.

[26] Tregambi C, Salatino P, Solimene R, Montagnaro F. An experimental characterization of Calcium Looping integrated with concentrated solar power. Chem Eng J 2018. doi:10.1016/j.cej.2017.08.068.

[27] Ortiz C, Valverde JM, Chacartegui R, Perez-Maqueda LA, Giménez P. The Calcium-Looping (CaCO3/CaO) process for thermochemical energy storage in Concentrating Solar Power plants. Renew Sustain Energy Rev 2019. doi:10.1016/j.rser.2019.109252.

[28] Rhodes NR, Barde A, Randhir K, Li L, Hahn DW, Mei R, et al. Solar Thermochemical Energy Storage Through Carbonation Cycles of SrCO 3 / SrO Supported on SrZrO 3 2015:3793–8. doi:10.1002/cssc.201501023.

[29] Ortiz C, Chacartegui R, Valverde JM, Becerra JA. A new integration model of the calcium looping technology into coal fired power plants for CO2capture. Appl Energy 2016;169:408–20. doi:10.1016/j.apenergy.2016.02.050.

[30] Benitez-Guerrero M, Valverde JM, Sanchez-Jimenez PE, Perejon A, Perez-Maqueda LA. Multicycle activity of natural CaCO3 minerals for thermochemical energy storage in Concentrated Solar Power plants. Sol Energy 2017. doi:10.1016/j.solener.2017.05.068.

[31] Da Y, Xuan Y, Teng L, Zhang K, Liu X, Ding Y. Calcium-based composites for direct solar-thermal conversion and thermochemical energy storage. Chem Eng J 2020. doi:10.1016/j.cej.2019.122815.

[32] Sarrión B, Perejón A, Sánchez-Jiménez PE, Pérez-Maqueda LA, Valverde JM. Role of calcium looping conditions on the performance of natural and synthetic Ca-based materials for energy storage. J CO2 Util 2018. doi:10.1016/j.jcou.2018.10.018.

[33] SOCRATCES Project. Fact Sheet. Solar calcium-looping integration for thermo-chemical energy storage. 2020.

[34] SOCRATCES Project. Deliverable 3.2. SOlar Calcium-looping integRAtion for Thermo-Chemical Energy Storage. 2020.

[35] Bhatia SK, Perlmutter DD. Effect of the product layer on the kinetics of the CO2-lime reaction. AIChE J 1983;29:79–86. doi:10.1002/aic.690290111.

[36] Gavalas GR. A random capillary model with application to char gasification at chemically controlled rates. AIChE J 1980;26:577–85. doi:10.1002/aic.690260408.

[37] Borgwardt RH. Calcination kinetics and surface area of dispersed limestone particles. AIChE J 1985;31:103–11. doi:10.1002/aic.690310112.

[38] Kendall M, Moran PAP. Geometrical probability. New York: Hafner Pub. Co.; 1963.

[39] García-Labiano F, Abad A, de Diego LF, Gayán P, Adánez J. Calcination of calcium-based sorbents at pressure in a broad range of CO2 concentrations. Chem Eng Sci 2002;57:2381–93. doi:10.1016/S0009-2509(02)00137-9.

[40] Wen CY, Chaung TZ. Entrainment Coal Gasification Modeling. Ind Eng Chem Process Des Dev 1979;18:684–95. doi:10.1021/i260072a020.

[41] Nellis G, Klein S. Heat transfer. Cambridge University Press; 2008.

[42] Hodgson P, Sceats M, Vincent A, Rennie D, Fennell P, Hills T. Direct Separation

Calcination Technology for Carbon Capture: Demonstrating a Low Cost Solution for the Lime and Cement Industries in the LEILAC Project. 14th Int Conf Greenh Gas Control Technol GHGT-14 2018. https://papers.ssrn.com/sol3/papers.cfm?abstract_id=3365844#%23 (accessed November 27, 2019).

[43] Martínez A, Pröll T, Romeo LM. Lime enhanced biomass gasification. Energy penalty reduction by solids preheating in the calciner. Int J Hydrogen Energy 2012;37. doi:10.1016/j.ijhydene.2012.08.002.

[44] Ylätalo J, Ritvanen J, Arias B, Tynjälä T, Hyppänen T. 1-Dimensional modelling and simulation of the calcium looping process. Int J Greenh Gas Control 2012;9:130–5. doi:10.1016/j.ijggc.2012.03.008.

[45] Moumin G, Ryssel M, Zhao L, Markewitz P, Sattler C, Robinius M, et al. CO2 emission reduction in the cement industry by using a solar calciner. Renew Energy 2020;145:1578–96. doi:10.1016/j.renene.2019.07.045.